M. Nastasi
J.W. Mayer

Ion Implantation and Synthesis of Materials

Springer

Ion Implantation and Synthesis of Materials

M. Nastasi J.W. Mayer

Ion Implantation and Synthesis of Materials

With 131 Figures and 10 Tables

Springer

Michael Nastasi, PhD
Laboratory Fellow and Team Leader
Ion-Solid Interaction and Interface Engineering Team
Los Alamos National Laboratory, MS-K771
Los Alamos NM 87545, USA
E-mail: nasty@lanl.gov

James W. Mayer, PhD
Center for Solid State Science
Arizona State University
Tempe, AZ, 85287-1704, USA
E-mail: james.mayer@asu.edu

Library of Congress Control Number: 2006930120

ISBN-10 3-540-23674-0 Springer Berlin Heidelberg New York
ISBN-13 978-3-540-23674-0 Springer Berlin Heidelberg New York

Springer is a part of Springer Science+Business Media.

springer.com

Typesetting by the Authors and SPi
Cover design: *design & production* GmbH, Heidelberg

Printed on acid-free paper SPIN 10864147 57/3100/SPi 5 4 3 2 1 0

To our loved ones

Preface

Ion implantation is one of the key processing steps in silicon-integrated circuit technology. Some integrated circuits require up to 35 implantation steps, and circuits are seldom processed with fewer than 10 implantation steps. Controlled doping at controlled depths is an essential feature of implantation. Ion beam processing can also be used to improve corrosion resistance, harden surfaces, reduce wear and, in general, improve materials properties. This book presents the physics and materials science of ion implantation and ion synthesis of materials with an emphasis on electronic materials. It covers ion-solid interactions used to predict ion ranges, ion straggling, and lattice damage. Also treated are the applications of ion implantation in the formation of integrated circuits and the slicing of silicon with hydrogen ion beams. Topics important for materials modification, such as ion beam-induced epitaxial growth of amorphous layers, ion-beam mixing, and sputtering, are also described.

This text is designed for undergraduate seniors and graduate students interested in electronic devices, surface engineering, reactor and nuclear engineering, and material science issues associated with irradiation effects in materials. The original course was offered by the Department of Materials Engineering. Approximately half the students came from electrical engineering or disciplines other than materials engineering. Their backgrounds and training varied. Hence, a firm grasp of the underlying concepts of ion-solid interactions in solids needed in the course could not be assumed. For this reason the first four chapters of the book are devoted to review of topics on particle interactions, binary collisions, and collision cross-sections. The purpose of these chapters is to provide sufficient coverage of the fundamentals for the subsequent chapters.

In writing this book, we have benefited immensely from the help of students in our classes. Their inquiries and responses to our lectures have strengthened the contents and organization of the book. Ms. Linda Woods is sincerely acknowledged for formatting and editing the book. We also thank Tobias Höchbauer for his contributions to Chapter 10, Lin Shao for his contributions to Chapter 14, and the ion implanter development scientists at Axcelis Technologies, Inc for their contributions to Chapter 15.

Los Alamos, Tempe — *Michael Nastasi*
June 2006 — *James W. Mayer*

Contents

1 General Features and Fundamental Concepts

1.1 Introduction

Ion beam processing of materials results from the introduction of atoms into the surface layer of a solid substrate by bombardment of the solid with ions in the electron-volt to mega-electron-volt energy range. The solid-state aspects are particularly broad because of the range of physical properties that are sensitive to the presence of a trace amount of foreign atoms. Mechanical, electrical, optical, magnetic, and superconducting properties all are affected by, and indeed may even be dominated by, the presence of such foreign atoms. The use of energetic ions affords the possibility of introducing a wide range of atomic species, independent of thermodynamic factors, thus making it possible to obtain impurity concentrations and distributions of particular interest; in many cases, these distributions would not otherwise be attainable.

Recent interest in ion beam processing has focused on studies of ion implantation, ion beam mixing, ion-induced phase transformations, and ion beam deposition. These interests have been stimulated by the possibilities of synthesizing novel materials with potential applications in the semiconductor, tribological, corrosion, and optical fields.

Ion beam processing provides an alternative and non-equilibrium method of introducing dopant atoms into the lattice. In typical applications, a beam of dopant ions is accelerated through a potential of 10–100 kV. The implantation system shown in Fig. 1.1 illustrates the basic elements required in this technique: ion source, acceleration column, mass-separator, and target chamber. With different types of ion sources available, a wide variety of beams may be produced with sufficient intensity for implantation purposes for integrated circuit technology; 10^{14}–10^{15} ions cm^{-2} (less than a 'monolayer'; see Sect. 1.4) is a representative ion dose. *Ion dose* is defined as the number of ions cm^{-2} implanted into the sample. Alternatively, the term *fluence* is used instead of dose. The ion beam current density is expressed in units of A cm^{-2}. The dose rate or flux is given in units of ions s^{-1} cm^{-2}.

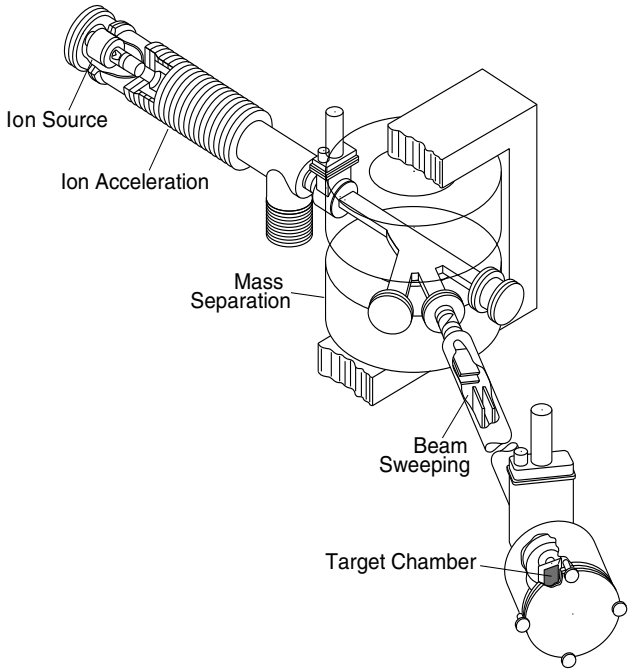

Fig. 1.1. Schematic drawing of an ion implantation system. A mass-separating magnet is used to select the ion species (elements and isotopes) of interest. Beam-sweeping facilities are required for large-area uniform implantations

1.2 Range Distributions

One of the most important considerations in any description of ion–solid interactions is the depth (range) distribution of the implanted ions. A large amount of experimental and theoretical work has been devoted to the task of understanding the energy-loss processes that govern the range distribution, and it is now possible to predict fairly accurately most of the factors involved. For example, a typical range distribution in an amorphous substrate from monoenergetic ions at moderate ion doses is approximately Gaussian in shape and may therefore be characterized by a projected range, R_p, and a straggling, ΔR_p, about this mean value, as depicted in Fig. 1.2. The notation uses Z and M for atomic number and atomic mass, respectively, with subscript 1 denoting the incident ions (Z_1, M_1) and subscript 2 denoting the ion-bombarded sample (or target). By convention, the energy of the incident ion is denoted by E_0 or by E without a subscript.

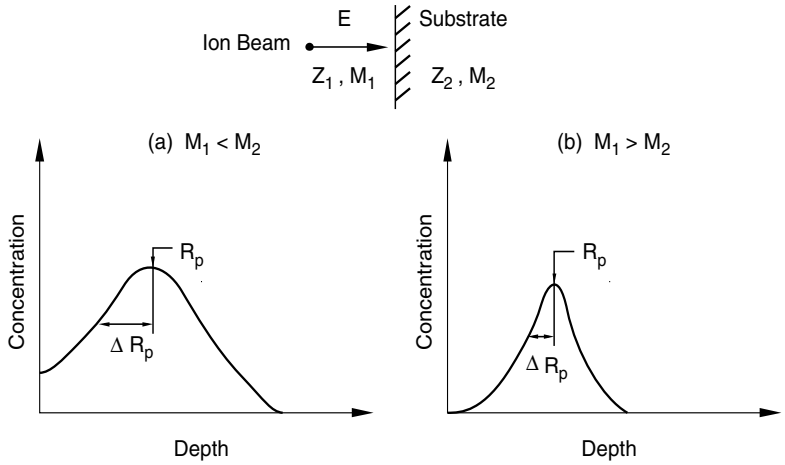

Fig. 1.2. The depth distribution of implanted atoms in an amorphous target for the cases in which the ion mass is (**a**) less than the mass of the substrate atoms or (**b**) greater than the mass of the substrate atoms. To a first approximation, the mean depth, R_p, depends on ion mass, M_1, and incident energy, E, whereas the relative width, $\Delta R_p/R_p$, of the distribution depends primarily on the ratio between ion mass and the mass of the substrate ion, M_2

1.3 Lattice Disorder

Lattice disorder and radiation-damage effects are produced in the substrate by the incident ion. As an implanted ion slows down and comes to rest, it has many violent collisions with lattice atoms, displacing them from their lattice sites. These displaced atoms can in turn displace others, and the net result is the production of a highly disordered region around the path of the ion, as shown schematically in Fig. 1.3 for the case of a heavy implanted atom at typically 10–100 keV. At sufficiently high doses, these individual disordered regions may overlap, and an amorphous or metastable crystalline layer may form.

Figure 1.4 shows the schematic atomic arrangement for a crystalline solid (a) and an amorphous solid (b). A crystalline solid has long-range atomic order; an amorphous solid has short-range order (the order among the nearest neighbors) but no long-range order. In a single-crystal, the entire sample is composed of atoms placed on well-defined planes and rows. Figure 1.5a shows a side view of a single-crystal, in which the planes of atoms are depicted by parallel pairs of lines. A polycrystalline sample is made of small single-crystal regions called crystallites, the planes and atomic rows of which are misaligned with respect to those in neighboring crystallites. A polycrystalline layer on a single-crystal substrate is shown in Fig. 1.5b.

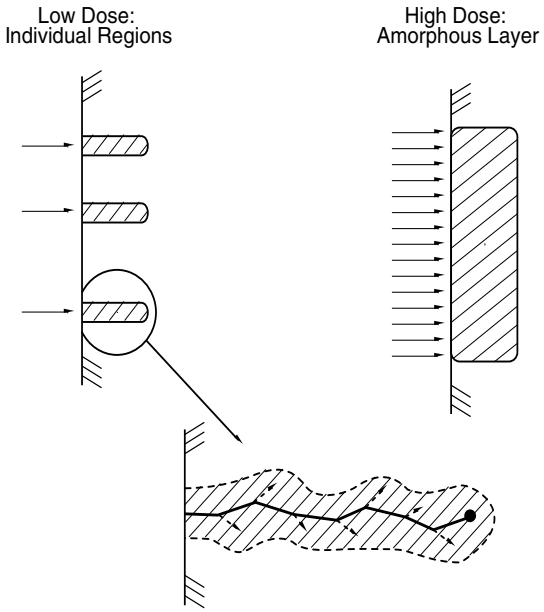

Fig. 1.3. A schematic representation of the disorder produced in room-temperature implantations of heavy ions at energies of 10–100 keV. At low doses, the highly disordered regions around the tracks of the ions are spatially separated from each other. The volume of the disordered region is determined primarily by the stopping point of the ion and the range of the displaced lattice atoms (*dashed arrows*). At high doses, the disordered regions can overlap to form an amorphous layer

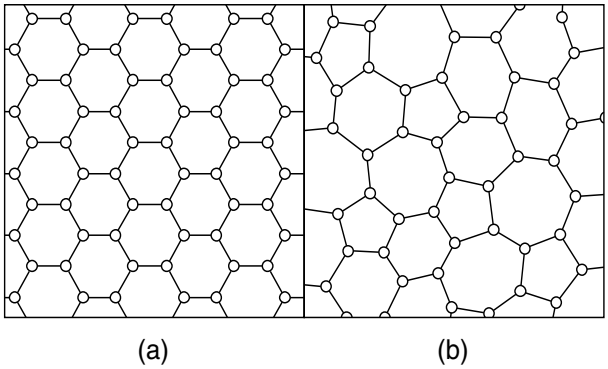

Fig. 1.4. Schematic atomic arrangement of (**a**) a crystalline solid and (**b**) an amorphous solid

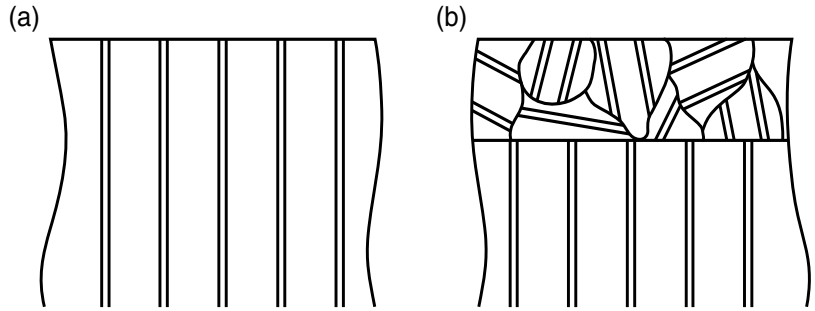

Fig. 1.5. Schematic representation for (**a**) a single-crystal with crystallographic planes perpendicular to the surface and (**b**) a polycrystalline layer on a single-crystal

1.4 Atomic and Planar Densities

To understand the description of ion implantation and ion doses, one must know the atomic density interplanar distance between planes and the number of atoms cm^{-2} on a given plane. In cubic systems with an atomic density of N atoms cm^{-3}, the crystal lattice parameter, a_c, is given by

$$a_\mathrm{c} = \left(\frac{\text{atoms/unit cell}}{N} \right)^{1/3}, \tag{1.1}$$

where, for systems with one atom per lattice point, there are four atoms per unit cell for a face-centered-cubic lattice (Al, Ag, Au, Pd, Pt) and there are eight for the common semiconductors germanium (Ge) and silicon (Si), which have the diamond cubic structure. Aluminum has an atomic density of 6.02×10^{22} atoms cm^{-3}, so that the lattice parameter is

$$a_\mathrm{c} = \left(\frac{4}{6.02 \times 10^{22}} \right)^{1/3} = 4.05 \times 10^{-8} \text{ cm}. \tag{1.2}$$

The atomic volume can be calculated without the use of crystallography. The atomic density N of atoms cm^{-3} is given by

$$N = \frac{N_\mathrm{A}}{A} \rho, \tag{1.3}$$

where N_A is Avogadro's number, ρ is the mass density in g cm^{-3}, and A is the atomic mass number. Taking Al as an example, where ρ is 2.7 g cm^{-3} and A is 27, the atomic density is $N = (6.02 \times 10^{23} \times 2.70)/27 = 6.02 \times 10^{22}$ atoms cm^{-3}. The semiconductors Ge and Si have atomic densities of about 4.4×10^{22} and 5.0×10^{22} atoms cm^{-3}, respectively. Metals such as Co, Ni, and Cu have densities of about 9×10^{22} atoms cm^{-3}. The volume Ω_V occupied by an atom is given by

$$\Omega_V = \frac{1}{N} \tag{1.4}$$

with a typical value of 20×10^{-24} cm^3.

The average areal density of a monolayer, N_s atoms cm^{-2}, also can be estimated without the use of crystallography by taking the atomic density N to the 2/3 power.

$$N_s \cong N^{2/3}. \tag{1.5}$$

Equation (1.5) gives the average areal density of one monolayer for a material with an atomic density N.

1.5 Energy and Particles

In the SI (or MKS) system of units, the joule (J) is a unit of energy, but the electron-volt (eV) is the traditional unit used in ion–solid interactions: we can define 1 eV as the kinetic energy gained by an electron accelerated through a potential difference of 1 V. The charge on the electron is 1.602×10^{-19} C, and a joule is a Coulomb-volt, so that the relationship between these units is given by

$$1\,\text{eV} = 1.602 \times 10^{-19}\,\text{J}. \tag{1.6}$$

Commonly used multiples of the electron-volt are the kilo-electron-volt (10^3 eV) and mega-electron-volt (10^6 eV).

In ion–solid interactions it is convenient to use cgs units rather than SI units in relations involving the charge on the electron. The usefulness of cgs units is clear when considering the Coulomb force between two charged particles with Z_1 and Z_2 units of electronic charge separated by a distance r

$$F = \frac{Z_1 Z_2 e^2 k_c}{r^2}, \tag{1.7}$$

where the Coulomb law constant $k_c = ¼\,\pi\varepsilon_0 = 8.988 \times 10^9$ m F^{-1} in the SI system (where 1 F ≡ 1 A s V^{-1}) and is equal to unity in the cgs system.

The conversion factor follows from:

$$e^2 k_c = (1.6\times10^{-19}\ \text{C})^2 \times 8.988\times10^9\ \text{m F}^{-1} = 2.3\times10^{-28}\ \text{C}^2\ \text{m F}^{-1}.$$

The conversions 1 C ≡ 1 A s and 1 J ≡ 1 C V lead to the units of the farad:

$$1\ \text{F} \equiv 1\ \text{A s V}^{-1},$$

so that

$$1\text{C}^2\ \text{m F}^{-1} \equiv 1\text{C}^2\ \text{V m (A s)}^{-1} \equiv 1\text{J m} \equiv 10^9\ \text{J nm} \equiv \frac{10^9\ \text{J nm}}{(1.6\times10^{-19}\ \text{J eV}^{-1})} = \frac{10^{28}}{1.6}\ \text{eV nm}$$

and

$$e^2 k_c = 2.31\times10^{-28}\ \text{C}^2\ \text{m F}^{-1} = \frac{2.31}{1.6}\ \text{eV nm} = 1.44\ \text{eV nm}.$$

In this book we will follow the cgs units for e^2 with $k_c = 1$, so that

$$e^2 = 1.44\ \text{eV nm}. \tag{1.8}$$

Each nucleus is characterized by a definite atomic number Z and mass number A; for clarity, we use the symbol M to denote the atomic mass in kinematic equations. The atomic number Z is the number of protons, and hence the number of electrons, in the neutral atom; it reflects the atomic properties of the atom. The mass number gives the number of nucleons (protons and neutrons); isotopes are nuclei (often called nuclides) with the same Z and different A. The current practice is to represent each nucleus by the chemical name with the mass number as a superscript, e.g., ^{12}C. The chemical atomic weight (or atomic mass) of elements as listed in the periodic table gives the average mass, i.e., the average of the stable isotopes weighted by their abundance. Carbon, for example, has an atomic weight of 12.011, which reflects the 1.1% abundance of ^{13}C.

The masses of particles may be expressed as given in Table 1.1 in terms of energy through the Einstein relation

$$E = Mc^2, \tag{1.9}$$

Table 1.1. Mass energies of particles and light nuclei

Particle	Symbol	Atomic mass (u)	Mass (10^{-27} kg)	Mass energy (MeV)
Electron	e or e^-	0.000549	9.1095×10^{-4}	0.511
Proton	p or $^1H^+$	1.007276	1.6726	938.3
Atomic mass unit (amu)	u	1.00000	1.6606	931.7
Neutron	n	1.008665	1.6747	939.6
Deuteron	D or $^2H^+$	2.01410	3.3429	1875.6
Alpha	α or $^4He^{2+}$	4.00260	6.6435	3727.4

which associates 1 J of energy with $1/c^2$ of mass, where c is the velocity of light, $c = 2.998 \times 10^8$ m s^{-1}. The mass of an electron, m_e, is 9.11×10^{-31} kg, which is equivalent to an energy

$$E = (9.11\times10^{-31}\,\text{kg})(2.998\times10^{8}\,\text{m s}^{-1})^2 = 8.188\times10^{-14}\,\text{J} = 0.511\,\text{MeV}. \tag{1.10}$$

The Einstein relation is also useful when calculating the velocity, v, of an ion of mass M and energy E,

$$v = \left(\frac{2E}{M}\right)^{1/2} = c\left(\frac{2E}{Mc^2}\right)^{1/2}. \tag{1.11}$$

For example, the velocity of a 2 MeV ^{4}He ion is

$$v = 3\times10^{8}\,\text{m s}^{-1}\left(\frac{2\times2\times10^{6}(\text{eV})}{3,727\times10^{6}(\text{eV})}\right)^{1/2} = 9.8\times10^{6}\,\text{m s}^{-1}.$$

1.6 The Bohr Velocity and Radius

The Bohr atom provides useful relations for simple estimates of atomic parameters. The Bohr radius is defined as the distance of the ground state electron from the nucleus in a hydrogen atom. The Bohr radius of the hydrogen atom is given by

$$a_0 = \frac{\hbar^2}{m_e e^2} = 0.5292 \times 10^{-8}\ \text{cm} = 0.05292\,\text{nm} \tag{1.12}$$

and the Bohr velocity of the electron in this orbit is

$$v_0 = \frac{\hbar}{m_e a_0} = \frac{e^2}{\hbar} = 2.188 \times 10^8\ \text{cm s}^{-1}, \tag{1.13}$$

where $\hbar = h/2\pi$ with Planck's constant $h = 4.136 \times 10^{-15}$ eV s. For comparison with the Bohr radius, the radius of a nucleus is given by the empirical formula

$$R = R_0 A^{1/3}, \tag{1.14}$$

where A is the mass number and R_0 is a constant equal to 1.4×10^{-13} cm. The nuclear radius is about four orders of magnitude smaller than the Bohr radius.

Suggested Reading

Cullity, B.D.: Elements of X-Ray Diffraction. Addison-Wesley Publishing Company, Boston, MA (1978)

Feldman, L.C., Mayer, J.W.: Fundamentals of Surface and Thin Film Analysis. North-Holland, New York (1986)

Mayer, J.W., Lau, S.S.: Electronic Materials Science. Macmillan, New York (1990)

Mayer, J.W., Eriksson, L., Davies J.A.: Ion Implantation in Semiconductors. Academic, New York (1970)

Nastasi, M., Mayer, J.W., Hirvonen, J.K.: Ion–Solid Interactions: Fundamentals and Applications. Cambridge University Press, Cambridge (1996)

Omar, M.A.: Elementary Solid-State Physics: Principles and Applications. Addison-Wesley Publishing Company, Boston, MA (1975)

Rimini, E.: Ion Implantation: Basics to Device Fabrication. Kluwer, Boston (1995)

Tu, K.N., Mayer, J.W., Feldman, L.C. Electronic Thin Film Science. MacMillan Publishing Company, New York (1992)

Weidner, R.T., Sells, R.L.: Elementary Modern Physics, 3rd edn. Allyn & Bacon, Boston, MA (1980)

Problems

1.1 Aluminum is a face-centered-cubic with a mass density of 2.70 g cm^{-3}
(a) Calculate the atomic density using (1.3)

(b) Calculate the average areal density using (1.5)
(c) What is the atomic volume?

1.2 For the canonical value of 10^{15} atoms cm^{-2} in a monolayer on a cubic crystal, estimate
(a) The bulk density
(b) The volume Ω_V occupied by an atom

1.3 Nickel is a face-centered-cubic metal with an atomic density of 9.14×10^{22} atoms cm^{-3}, an atomic weight of 8.7, and density of 8.91 g cm^{-3}
(a) What is the lattice parameter, a_c, and the atomic volume, Ω_V?

1.4 Silicon has a diamond cubic lattice structure with an atomic density of 5×10^{22} atoms cm^{-3}, an atomic weight of 28.09 and a density of 2.33 g cm^{-3}
(a) What are silicon's lattice parameter and atomic volume, Ω_V?

1.5 Calculate the energy in eV of a proton moving at the Bohr velocity. What is the velocity of a 35 keV A s ion?

2 Particle Interactions

2.1 Introduction

The manner in which the potential energy of a two-particle system varies with the distance separating the two centers determines both the equilibrium properties of an assembly of atoms and the way that energetic particles interact with a lattice of stationary atoms. The scattering probability of an ion–atom collision is intimately related to the interaction forces between atoms.

2.2 Interatomic Forces

We start our discussion with the concept that atoms are comprised of a central nucleus and orbital electrons, and we consider the forces when one atom interacts with another atom. The nucleus is effectively a solid body of diameter $\sim 10^{-12}$ cm with a positive charge, Z, which is dependent on the number of protons present. If there were no orbital electrons, the force between two nuclei separated by a distance r would be Coulombic, of the form

$$F(r) = \frac{Z_1 Z_2 e^2}{r^2}, \tag{2.1}$$

where Z_1 and Z_2 are the numbers of protons contained in the nucleus, and $e^2 = 1.44$ eV nm (1.8).

For most purposes, the force between two atoms is expressed in terms of an interatomic potential, which depends primarily on the separation, r, between the atoms or other charged particles. If the dependence of the potential on other coordinates is neglected (central force approximation), then the force, $F(r)$, and the potential, $V(r)$, are related by

$$F(r) = -\frac{\mathrm{d}}{\mathrm{d}r}[V(r)]. \tag{2.2}$$

The restriction to r-dependence is usually a good approximation. Throughout this text, the variable r will define the separation distance between two interacting particles. The pairs might be atom–atom, electron–atom, electron–electron, ion–atom, etc.

The potential energy, or binding energy, of a single atom is the work done in bringing all components of the atom from infinity to their equilibrium positions in the atom. The simplest example is the semiclassical picture of the hydrogen atom. Thus, if an electron or charge, e, is brought from infinity to a distance r from the center of a proton under the attractive Coulomb field, the (negative) potential energy would be

$$V_{\mathrm{a}}(r) = \int_{\infty}^{r} \left(\frac{e^2}{r^2} \right) \mathrm{d}r = -(e^2 / r). \tag{2.3}$$

2.3 Short- and Long-Range Interatomic Forces

There are different types of forces that make up the interaction between two atoms over a large range of separation. Both experimental phenomena and theoretical considerations suggest that the forces can be categorized as *short-* and *long-range* forces.

The nature of the long-range force depends on whether the system consists of neutral atoms, charged ions, or a combination of the two. The force of greatest magnitude at large separations is the Coulomb electrostatic interaction between two charged ions, assumed to be point charges. The Coulomb potential is obtained by applying (2.2) to (2.1) to give

$$V_{\mathrm{c}}(r) = -\left(\frac{Z_1 Z_2 e^2}{r} \right). \tag{2.4}$$

where $Z_1 e$ and $Z_2 e$ are the charges of the ions. From (2.2) we see that the force $F(r)$ for a given central force field is expressed in terms of the interaction potential by

$$V_{\mathrm{c}}(r) = \int_{r}^{\infty} F(r) \mathrm{d}r. \tag{2.5}$$

If one or both of the particles are neutral, this Coulomb force is zero in the two-body approximation, and the long-range interaction is greatly reduced.

As two atoms approach each other, some degree of *merging* of the particles occurs. As the particles merge, the electron orbits from the electrons of each atom begin to overlap, and a limitation in the occupation of available electron states arises due to the Pauli Exclusion Principle. Under such circumstances, the

quantum mechanically derived short-range forces begin to govern the interaction potential, and the simple picture presented by the long-range Coulombic potential is no longer valid.

2.4 Interatomic Forces in Solids

In many applications involving the use of interatomic potentials in physics and materials science, it is not necessary to know the precise form of the force field between the interacting particles. Even if the exact functional form of the potential energy were known, its mathematical complexity would restrict it from being used in simple analytical work, finding utility only in detailed computer calculations. Empirical atomic interactions are based on a simple analytical model, which provides a mathematically tractable, analytical expression for the pairwise interaction between two atoms or ions.

A useful potential in modeling the condensed states of solids or liquids is the Lennard-Jones potential

$$V(r) = \frac{pq}{p-q}\Delta E\left[\frac{1}{p}\left(\frac{r_0}{r}\right)^p - \frac{1}{q}\left(\frac{r_0}{r}\right)^q\right], \tag{2.6}$$

where r_0 is the equilibrium interatomic separation between nearest neighbors (and is typically of the order of 10^{-8} cm), $\Delta E = V(r_0)$, and p and q are fitting constants.

Figure 2.1a schematically shows the potential energy diagram for a solid. While the exact features of this curve are model-dependent, the general shape and trends are universal for all materials. The minimum energy in this curve corresponds to the most stable configuration for atom spacing and represents the maximum energy that must be applied to pull an atom free from the crystal, i.e., the cohesive energy of the solid. The distance r_0, which is located at the minimum in the energy curve, corresponds to the equilibrium distance between atom near neighbors. The fact that such an equilibrium distance exists implies that the potential energy of the system possesses a minimum, at which point there are no net forces on the atoms. As Fig. 2.1 shows, any departure from r_0 that represents a decrease or increase in the spacing between atoms away from the equilibrium spacing results in an increase in the energy of the material (less negative) and makes the material less stable.

An alternative way to look at Fig. 2.1a is to recall that $-\mathrm{d}V/\mathrm{d}r = F$, where F is the force relationship between the atoms in the crystal. Note that under this convention, a positive force results when dr is negative, and a negative force results when dr is positive, which is opposite to the stress convention applied in materials science. We plot $F = \mathrm{d}V/\mathrm{d}r$ in Fig. 2.1b to maintain the stress convention, wherein increasing the distance between atoms produces a positive restoring force,

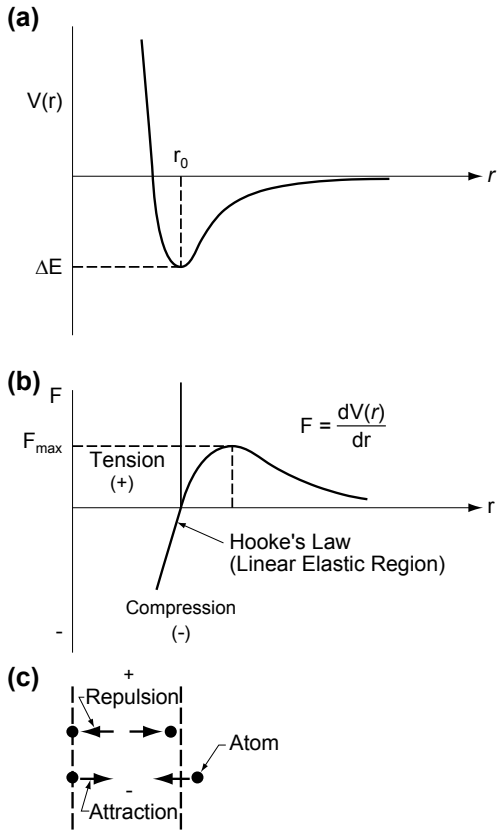

Fig. 2.1. (**a**) Interatomic potential function, $V(r)$, plotted against interatomic distance, r. (**b**) Interatomic force plotted as a function of r. (**c**) A schematic showing the force neighboring atoms experience as a function of separation (Tu et al. 1992)

and compressing the spacing produces a repulsive force. This data shows that there are no forces acting on atoms at a spacing of r_0. (The directions of the forces that an atom near the minimum experiences due to a neighboring atom located at $r = 0$ are indicated in Fig. 2.1c.) If the atoms are displaced toward each other, a repulsive force acts to increase the interatomic distance back to r_0. On the other hand, if the distance between atoms is increased, an attractive force acts to decrease the interatomic distance.

For crystalline solids, the equilibrium interatomic distance, r_0, can be estimated from knowledge of lattice site separation distances and is typically expressed as some fraction of the lattice parameter a_c. Aluminum forms a face-centered-cubic (fcc) lattice, with lattice parameter $a_c = 0.405$ nm. Since the densest packing direction is along the face diagonal, i.e., along the ⟨110⟩ direction, the equilibrium interatomic distance in Al is $\sqrt{2}a_c/2 = 0.29\text{nm}$. We can also calculate the distance approximately from the atomic volume Ω_v, where Ω_v is the reciprocal of the atomic

density N in atoms cm^{-3} ($\Omega_v = 1/N$; $\Omega_v = a^3/4$ for fcc lattices). The equilibrium distance $r_0 \cong \Omega^{1/3} = 0.26$ nm in this approximation.

2.5 Energetic Collisions of Atoms and Ions and the Screened Coulomb Potential

We now pass from the interactions between those atoms in equilibrium to the interactions between particles whose energies and velocities exceed that of thermal motion. This brings us to the range of interatomic forces at distances less than the equilibrium distance, r_0, in solids. The interaction distance, r, during the collision will depend on the relative energy of the collision. Consequently, some amount of closed-shell interpenetration and overlap will occur, which, in turn, will lead to considerable modification of the particle wave function at the moment of impact. Clearly, knowledge of the interatomic potential at small separations is crucial to the solution of problems involving ion–solid interactions and radiation damage in solids. The manner in which the potential energy of a two-particle system varies with the distance separating the two centers determines both the equilibrium properties of an assembly of atoms and the way that energetic particles interact with a lattice of stationary atoms. In the area of ion–solid interactions, knowledge of the potential energy function is necessary to determine the rate at which energetic ions lose energy as they penetrate a solid.

As an introduction to the problem of the interaction of an energetic ion with atoms in a solid, we first consider the limits of the collision. Consider two atoms with masses M_1 and M_2 and atomic numbers Z_1 and Z_2, respectively, separated by a distance r. The force is best described by a potential energy, $V(r)$, which arises from many-body interactions involving the electrons and the nuclei.

There are two useful reference points in the scale of separation. The first is the Bohr radius of the hydrogen atom, $a_0 = 0.053$ nm, which gives an indication of the extent of the atomic electron shells. The second is r_0, the spacing between neighboring atoms in the crystal (typically 0.25 nm). For the extreme condition, where $r >> r_0$, the electrons populate the energy levels of the individual atoms, and, from the Pauli exclusion principle, there is a maximum number that can occupy any set of levels. The lowest levels, corresponding to the inner closed-shells, all will be occupied, and there will only be empty levels in the outer valence shells. As two atoms are brought together, the valence shells will begin to overlap, and there may be attractive interactions of the type that form bonds. Under these conditions the Lennard-Jones potential reasonably approximates the atomic interaction.

At the other extreme, when $r << a_0$, the nuclei become the closest pair of charged particles in the system, and their Coulomb potential dominates all other terms in $V(r)$. Then

$$V(r) = \frac{Z_1 Z_2 e^2}{r}, \tag{2.7}$$

where $e^2 = 1.44$ eV nm.

However, at intermediate distances, when $a_0 < r < r_0$, a positive potential energy of interaction results in a repulsive force between the two atoms. The main contributions to this potential are: (1) the electrostatic repulsion between the positively charged nuclei, and (2) the increase in energy required to maintain the electrons of nearby atoms in the same region of space without violating the Pauli exclusion principle. Since no two electrons can occupy the same position, overlapping of electrons from two atoms must be accompanied by promotion of some of the electrons to higher, unoccupied levels of the atomic structure. The energy required for this process increases as the atoms approach each other, because a large number of the orbital electrons become affected. Thus, for intermediate distances, there is a reduction of the Coulomb potential because of the electrostatic screening of the nuclear charges by the space charge of the innermost electron shells. One then refers to a *screened Coulomb potential*. This potential is given by

$$V(r) = \frac{Z_1 Z_2 e^2}{r} \chi(r), \tag{2.8}$$

where $\chi(r)$ is the screening function and is defined as the ratio of the actual atomic potential, at some radius r, to the Coulomb potential.

In ideal circumstances, $\chi(r)$ properly moderates the Coulomb potential to describe the interaction between ions and atoms at all separation distances. For large distances, $\chi(r)$ should tend to zero, while for very small distances, $\chi(r)$ should tend to unity. Such features allow a *single* interatomic potential energy function, (2.8), to describe the entire collision process.

2.6 Screening Functions

In the relatively low-velocity collision regime of most ion–solid interactions used in ion implantation and other ion surface modification experiments, the typical ion–atom distance of closest approach falls in the regime of $a_0 < r < r_0$, so that the nuclear charge is screened by the electrons. The development of a screening function requires a model of the atom as a starting point. The simplest atomic models are statistical models that allow straight forward calculation of the charge distribution of the colliding atoms. The charge distributions obtained from classical models developed by Thomas–Fermi, Bohr, Lenz–Jensen, and Moliere scale simply with atomic number and do not include any shell structure information.

Simple mathematical expressions have been developed for the Thomas–Fermi, Bohr, Lenz–Jensen, and Moliere screening functions. Several forms exist for the Thomas–Fermi model. The earliest and best known of these is the Sommerfeld asymptotic form,

$$\chi(r) = \left\{1 + \left(\frac{r}{12^{2/3}}\right)^{0.772}\right\}^{-3.886}. \tag{2.9}$$

Lindhard and coworkers proposed two somewhat simpler and more approximative Thomas–Fermi screening functions given by

$$\chi(r) = 1 - \frac{r}{(3 + r^2)^{1/2}} \tag{2.10}$$

and

$$\chi(r) = 1 - 1/2r. \tag{2.11}$$

The Moliere form of the screening function is composed of three exponentials:

$$\chi(r) = 7p\exp(-qr) + 11p\exp(-4qr) + 2p\exp(-20qr). \tag{2.12}$$

The screening function for a Bohr atom with $x = r/a_{TF}$ is

$$\chi_{\text{Bohr}}(x) = \exp(-x), \tag{2.13}$$

and the screening function for a Lenz–Jensen atom is

$$\begin{aligned}\chi_{\text{LJ}}(r) = {} & [0.7466\exp(-1.038r)] + [0.2433\exp(-0.3876r)] \\ & + [0.01018\exp(-0.206r)].\end{aligned} \tag{2.14}$$

While classical models can be used to provide basic insight into screened interatomic potentials, the use of quantum mechanically derived charge distributions based on the Hartree–Fock atomic model create significant changes in the details of the interaction potential. In an attempt to find an analytic function that accurately predicts the interatomic potential between atoms, Ziegler, Biersack, and Littmark (ZBL; 1985) extended an earlier study made by Wilson et al. (1977), performing detailed calculations of solid-state interatomic potentials for 261 atom pairs. The details of the calculations can be found in Ziegler et al. (1985). The calculated total interaction potential was used together with the screening function, (2.8), to produce the universal screening function

$$\begin{aligned}\chi_{\text{U}} = {} & 0.1818\exp(-3.2x) + 0.5099\exp(-0.9423x) \\ & + 0.2802\exp(-0.4028x) + 0.02817\exp(-0.2016),\end{aligned} \tag{2.15}$$